Physica E 146 (2023) 115550

Contents lists available at ScienceDirect

Physica E: Low-dimensional Systems and Nanostructures

journal homepage: www.elsevier.com/locate/physe

The diagrammatic method of Berezinskii for one-dimensional disordered wire with spin–orbit interaction

Bahruz Suleymanli [a,*], Enver Nakhmedov [b], Farida Tatardar [b,c], Bilal Tanatar [d]

[a] Yildiz Technical University, Department of Physics, 34220, Esenler, Istanbul, Turkey
[b] Institute of Physics of National Academy of Sciences of Azerbaijan, H. Javid ave. 133, Baku, AZ-1143, Azerbaijan
[c] Khazar University, Mahsati str. 41, AZ 1096, Baku, Azerbaijan
[d] Department of Physics, Bilkent University, 06800 Ankara, Turkey

ARTICLE INFO

Keywords:
White-noise Gaussian random potential
Spin–orbit interaction
Electron density distribution

ABSTRACT

We extend Berezinskii's diagram technique to the one-dimensional disordered wire containing Rashba and Dresselhaus spin–orbit interactions. The retarded and advanced Green's functions are factorized in coordinates space in the presence of spin–orbit interactions. This factorization allows us to transform all coordinate dependence of the Green's functions from lines to the impurity vertices. Our calculations show that all possible impurity vertices giving a contribution to the correlators do not differ from those given in the conventional technique, except that they are written in a 2×2 matrix form and the Fermi velocity v_F^* now depends on the spin–orbit coupling constants. The diagrammatic method of Berezinskii with spin–orbit interaction is used to obtain the distribution of the electron density of the localized state $p_\infty(y)$.

1. Introduction

One of the essential problems in spintronics is how impurities affect the spin precession in the presence of spin–orbit interaction (SOI). Existence of a macroscopic structural inversion asymmetry or a bulk inversion asymmetry in a disordered 2D system was shown to change the sign of the phase-coherent localization correction to the conductivity [1–4], driving the system from a weak localization regime into an antilocalization one. The Rashba and Dresselhaus SO terms equally and independently contribute to the weak antilocalization correction. Generation of a dissipationless transverse spin current or a spin Hall current by a driving electric field was predicted [5,6] in a clean, infinite and homogeneous structural inversion asymmetric 2D system. Even an arbitrary small concentration of nonmagnetic impurities was shown [7–10] to suppress totally the universal value of the spin Hall conductivity.

Single dislocations in plastically deformed silicon [11,12] and atomic chains at semiconductor surface [13,14] are two classes of one dimensional samples, where the spin–orbit interaction mediated energy band splitting was observed. Although there is big activity in studies of Rashba-type SOI in 1D system [15–20], a scattering on impurities was considered only in few works [21,22]. It is necessary to mention that many interesting effects have been revealed [23] in a one channel (Aharonov–Bohm) ring by taking into account SOI.

The competition of the randomness and interaction effects in low dimensional systems is still one of the most intriguing problems even in the absence of the Rashba and Dresselhaus SOIs. Weak Coulomb interactions between electrons moving diffusively in a disordered system have been shown to increase the localization effect [24]. Interference between the propagated and backscattered electronic waves results in a localization. Localization in $1D$ structures was qualitatively studied by Mott and Twose [25] in the random Kronig–Penney model. They concluded that in a $1D$ system all electronic states with an arbitrary random field and with an arbitrary concentration of the randomness must be localized. A rigorous proof of this statement has been done later by Borland [26] and Halperin [27]. Indeed, for a weak randomness when the condition of $k_F l \gg 1$ or $\epsilon_F \tau_0 \gg 1$, with ϵ_F being the Fermi energy, is satisfied, the electron remains in the vicinity of the Fermi lever either at $p = p_F$ or at $p = -p_F$. Although a forward scattering on impurities with the mean free path l^+ cannot significantly change the character of electronic wave function, the backward scattering with the mean free path l^- forces the electron to scatter from p_F to $-p_F$ and back, escaping the electron in length scale of the order l^-. Therefore, the number of electrons passing the whole length of a sample with length of $L \gg l^-$ is exponentially small $\propto \exp(-L/l^-)$, because of the number of electron having a mean free path l larger than l^- is $\propto \exp(-l/l^-)$. Localization of the wave function in the regime of weak randomness, $\epsilon_F \tau_0 \gg 1$, is not expected to change the

* Corresponding author.
E-mail address: bahruz.suleymanli@gmail.com (B. Suleymanli).

https://doi.org/10.1016/j.physe.2022.115550
Received 28 August 2022; Received in revised form 17 October 2022; Accepted 22 October 2022
Available online 29 October 2022

density of electronic states (DOS) significantly, instead it changes the mobility or diffusion coefficient, and therefore the static conductivity of a system according to the Einstein relation for the conductivity $\sigma = e^2\rho_0^{(d)}D_d$, where $\rho_0^{(d)}(\epsilon_F) = mp_F^{d-2}/\hbar^2\pi^{1-d}$, D_d are the DOS and the diffusion coefficient d-dimensional electron gas, correspondingly. The high-frequency conductivity $\sigma(\omega)$ in a disordered $1D$ system occurs, according to the qualitative description of Mott [28,29], due to resonance hopping of electron between two localized states at distance x separated by the minimal energy difference $\Delta E = E_0\exp(-|x|/l^-)$, where E_0 is the amplitude of the high-frequency electric field $E = E_0\cos\omega t$. The energy absorption per unit time and unit length in the presence of ac-electric field is, from one hand, $\Delta\mathcal{E} = \frac{1}{2}\sigma(\omega)E_0^2$. On the other hand, the absorbed energy can be found by calculating the probability of an amplitude for transition from the localized level with energy ϵ_a to the level with energy ϵ_b, separated by the distance $|z_{ab}|$, as $2\pi\frac{1}{4}(eE_0)^2|z_{ab}|^2\rho_0^{(1d)}(\epsilon_b)$, and then multiplying the total probability, obtained by integrating this expression over all possible separation, to the number of electrons $\omega\rho_0^{(1d)}(\epsilon_b)$, participating in the absorption process in the energy interval $\omega = \epsilon_a - \epsilon_b$. From these two expressions for the absorption energy one gets

$$\sigma(\omega) \propto e^2\nu_1^2(\epsilon_F)\omega^2\int|z_{ab}|^2\,dz. \tag{1}$$

Taking into account the qualitative expression for the matrix elements $z_{ab} \sim z^2e^{-2|z|/l_-}$, and the lower limit of integration as $Z_c = 2l^-\ln(v_F/\omega l^-)$, one gets the following expression for the conductivity

$$\sigma(\omega) \propto e^2l^-\left(\omega l^-/v_F\right)^2\ln^2\left(\omega l^-/v_F\right). \tag{2}$$

The interference effects in 1D disordered systems are strong, and therefore, the diffusion approximation, which is used in higher dimensions (D > 1), is not acceptable (and applicable) in 1D system. Significant progress in the theory of a $1D$ weakly disordered system is connected with a real-space diagrammatic technique developed by Berezinskii [30]. By selection of the impurity vertices, which do not contain the strongly oscillating phase factors $\sim e^{\pm ip_Fy_j}$ at a location of the impurity y_j, Berezinskii derived the rigorous expression for the low-frequency asymptotics of the ac-conductivity of $1D$ weakly disordered system. In this paper, we show that the Berezinskii's technique is applicable in the presence of SOI in a 1D disordered system.

The rest of this paper is organized as follows. In the next Section formulation of the problem is presented. In Section 3, we introduce "bare" Green's functions describing a one-dimensional disordered wire containing Rashba and Dresselhaus SOIs. By applying the diagrammatic theory of Berezinskii [30] to the case of SOI in Section 4, we draw all possible impurity vertices and calculate them. The diagrammatic method of Berezinskii with SOI is used to obtain the distribution of the electron density of the localized state $p_\infty(y)$ in Section 5. Conclusions are given in Section 6. Some technical aspects of Berezinskii's diagram method are relegated to Appendix.

2. Model and formulation of the problem

We consider a one-dimensional disordered wire in the presence of Rashba and Dresselhaus spin–orbit couplings (SOCs). Hamiltonian for such a system reads

$$\hat{H} = \frac{\hat{P}_y}{2m^*} + \sum_j V(y-y_j) + \hat{H}_R + \hat{H}_D, \tag{3}$$

where m^* is an electron effective mass, $\hat{P}_y = \frac{\hbar}{i}\frac{\partial}{\partial y}$ is y-component of the momentum operator, $V(y-y_j)$ is the potential of an impurity located at point y_j, $\hat{H}_R$ and $\hat{H}_D$ represent Rashba and Dresselhaus SOIs, respectively. In a two-dimensional system, $\hat{H}_R^{2D} + \hat{H}_D^{2D}$ can be written as [31]

$$\hat{H}_R^{2D} + \hat{H}_D^{2D} = \frac{\alpha}{\hbar}\left(\sigma_x\hat{P}_y - \sigma_y\hat{P}_x\right) + \frac{\beta}{\hbar}\left(\sigma_x\hat{P}_x - \sigma_y\hat{P}_y\right), \tag{4}$$

where α and β are Rashba- and Dresselhaus- SOC constants, correspondingly, and σ_i with $i = x,\ y$ are the Pauli spin-matrix components

$$\sigma_x = \begin{pmatrix}0 & 1\\ 1 & 0\end{pmatrix}; \qquad \sigma_y = \begin{pmatrix}0 & -i\\ i & 0\end{pmatrix}. \tag{5}$$

In a quasi one-dimensional system with homogeneous spin–orbit interaction, by choosing the form of lateral confinement it is possible to express the contributions of Rashba and Dresselhaus SOIs (4) in two terms: the first one is the intersubband coupling term $\hat{H}_R^{mix} + \hat{H}_D^{mix}$ and the second one is the spin precession term $\hat{H}_R^{prec} + \hat{H}_R^{prec}$ [32]

$$\hat{H}_R^{mix} + \hat{H}_D^{mix} = -\frac{\alpha}{\hbar}\sigma_y\hat{P}_x + \frac{\beta}{\hbar}\sigma_x\hat{P}_x, \tag{6}$$

$$\hat{H}_R^{prec} + \hat{H}_D^{prec} = \frac{\alpha}{\hbar}\sigma_x\hat{P}_y - \frac{\beta}{\hbar}\sigma_y\hat{P}_y. \tag{7}$$

Since we consider a purely one-dimensional system, the mixing term vanishes [33] and only the precession term contributes to the Hamiltonian (3)

$$\hat{H}_R + \hat{H}_D = \frac{\alpha}{\hbar}\sigma_x\hat{P}_y - \frac{\beta}{\hbar}\sigma_y\hat{P}_y. \tag{8}$$

The correlation functions for the charge $j^0(y)$ and current $j^1(y)$ operators

$$j^0(y) = \psi^\dagger(y)\psi(y) \qquad \text{and} \qquad j^1(y) = \frac{\hbar^2}{2m}\left(\frac{\partial}{\partial y} - \frac{\partial}{\partial y'}\right)\psi^\dagger(y)\psi(y')|_{y=y'}. \tag{9}$$

Then, the correlation functions $\chi^a(y-y',\omega)$ are expressed

$$\begin{aligned}\chi^a(y-y',\omega) &= \int_0^\infty dt e^{i\omega t}\int dE f(E)\left\langle \mathrm{Tr}\ \delta_E j^a(y,t)j^a(y',t')\right\rangle\\ &= \int_{-\infty}^\infty\frac{dk}{2\pi}\chi^a(k,\omega)e^{ik(y-y')},\end{aligned} \tag{10}$$

where $f(E)$ is the distribution, and δ_E is the density matrix of the microcanonical distribution

$$\delta_E = \frac{1}{2\pi i}\left\{\frac{1}{E-\hat{H}-i0} - \frac{1}{E-\hat{H}+i0}\right\}. \tag{11}$$

By introducing the Green's functions $G^\pm(y,y'|E)$ for the energy E and $G'(y,y'|E+\omega)$ for the energy $E+\omega$ as

$$G^\pm(y,y'|E) = \frac{1}{E-\hat{H}\pm i0}, \qquad \text{and} \qquad G'(y,y'|E+\omega) = \frac{1}{E+\omega-\hat{H}}, \tag{12}$$

the correlators are expressed through the Green's functions

$$\chi_\pm^0(y-y') = \frac{1}{2\pi}\left\langle G^\pm(y,y'|E)G'(y',y|E+\omega)\right\rangle, \tag{13}$$

and

$$\begin{aligned}\chi_\pm^1(y-y'|E+\omega) = \frac{1}{2\pi}\Bigg\langle&\left(\frac{\partial}{\partial y_1} - \frac{\partial}{\partial y_2}\right)\left(\frac{\partial}{\partial y_1'} - \frac{\partial}{\partial y_2'}\right)\\ &\times G^\pm(y_1,y_1'|E)G'(y_2',y_2|E+\omega)\Bigg\rangle\Bigg|_{\substack{y_1=y_1'=y\\ y_2=y_2'=y'}}\end{aligned} \tag{14}$$

The unaveraged diagram for density–density or current–current correlator consists of two electron lines going from the point y' to y. Ordering the impurity locations $\{y_j\}$ between y and y', all coordinate dependence can be transferred from lines of Green's functions to the vertices. The central idea in Berezinskii's diagrammatic technique is that the "bare" Green's functions, the retarded $G_0^+(y,y')$ and advanced $G_0^-(y,y')$ functions, are factorized in coordinates space.

3. "Bare" Green's functions

The "bare" Hamiltonian in the absence of an external potential is written in the form

$$\hat{H}_0 = -\frac{\hbar^2}{2m^*}\frac{\partial^2}{\partial y^2} + \frac{\alpha}{\hbar}\sigma_x\hat{P}_y - \frac{\beta}{\hbar}\sigma_y\hat{P}_y, \tag{15}$$

In order to solve the Schrödinger equation $\hat{H}_0\boldsymbol{\Phi}_k(y) = \epsilon\boldsymbol{\Phi}_k(y)$ one uses the spinor wave-function as

$$\begin{aligned}\boldsymbol{\Phi}_k(y) &\equiv \langle y|k\rangle \\ &= \begin{pmatrix}\phi_k^{\uparrow}(y)\\ \phi_k^{\downarrow}(y)\end{pmatrix} \\ &= \begin{pmatrix}a\\ b\end{pmatrix}e^{iky},\end{aligned} \tag{16}$$

where a and b are constants. The energy spectrum ϵ can be found as a solution of the following determinant

$$\begin{vmatrix}\epsilon - \frac{\hbar^2k^2}{2m^*} & -(\alpha+i\beta)k\\ -(\alpha-i\beta)k & \epsilon - \frac{\hbar^2k^2}{2m^*}\end{vmatrix} = 0, \tag{17}$$

which yields

$$\epsilon(k) = \frac{\hbar^2k^2}{2m^*} \pm \sqrt{k^2(\alpha^2+\beta^2)}. \tag{18}$$

The coefficients a and b are determined from the normalization condition $|a|^2 + |b|^2 = 1$ and from the relation

$$\begin{aligned}\frac{b}{a} &= \frac{\epsilon - \frac{\hbar^2k^2}{2m^*}}{k(\alpha+i\beta)} \\ &= \frac{k(\alpha-i\beta)}{\epsilon - \frac{\hbar^2k^2}{2m^*}}.\end{aligned} \tag{19}$$

Now the eigenvector reads

$$\boldsymbol{\Phi}_k(y) = a\begin{pmatrix}1\\ \pm\sqrt{\frac{\alpha-i\beta}{\alpha+i\beta}}\frac{|k|}{k}\end{pmatrix}e^{iky}. \tag{20}$$

Green's function is defined as a solution of the following differential equation

$$[\epsilon - \hat{H}_0]G(y,y';\epsilon) = \delta(y-y'), \tag{21}$$

where $\hat{H}_0(y)\boldsymbol{\Phi}_k(y) = \lambda_k\boldsymbol{\Phi}_k(y)$. By writing $G(y,y';\epsilon) = \langle y|G(\epsilon)|y'\rangle$ and $\delta(y-y')\hat{H}_0(y) = \left\langle y|\hat{H}_0|y'\right\rangle$, the differential equation for the Green's function is rewritten as $(\epsilon - \hat{H}_0)G(\epsilon) = 1$, and one gets

$$\begin{aligned}G(\epsilon) &= \frac{1}{\epsilon - \hat{H}_0} \\ &= \sum_k \frac{|k\rangle\langle k|}{\epsilon - \hat{H}_0},\end{aligned} \tag{22}$$

or for $G(y,y';\epsilon)$

$$\begin{aligned}G(y,y';\epsilon) &= \left\langle y|G(\epsilon)|y'\right\rangle \\ &= \sum_k \frac{\langle y|k\rangle\langle k|y'\rangle}{\epsilon - \hat{H}_0}.\end{aligned} \tag{23}$$

The expression on the numerator seems to be the dyadic (or outer) product of the eigen-vectors

$$\begin{aligned}\langle y|k\rangle\left\langle k|y'\right\rangle &= \boldsymbol{\Phi}_k(y)\otimes\bar{\boldsymbol{\Phi}}_k(y') \\ &= |k\rangle\otimes\langle k|\cdot e^{ik(y-y')} \\ &= |a|^2\begin{pmatrix}1 & \pm\sqrt{\frac{\alpha-i\beta}{\alpha+i\beta}}\frac{|k|}{k}\\ \pm\sqrt{\frac{\alpha+i\beta}{\alpha-i\beta}}\frac{|k|}{k} & 1\end{pmatrix}\end{aligned} \tag{24}$$

"Bare" Green's functions for a free particle with energy ϵ propagating from point y to y' are written

$$\mathbb{G}^{\pm}(y,y'|\epsilon) = \int_{-\infty}^{\infty}\frac{dk}{2\pi}\frac{e^{ik(y-y')}}{\epsilon - \hat{H}_0 \pm i\delta} \tag{25}$$

where $\pm$ correspond to the retarded and advanced Green's functions, δ is an infinitesimal. The denominator $\mathbf{M} = \epsilon - \hat{H}_0 \pm i\delta$ is 2×2 matrix. By multiplying it to the reverse matrix $\mathbf{M}^{-1}$ with $\mathbf{M}\mathbf{M}^{-1} = \hat{I}$ yields

$$\mathbb{G}^{\pm}(y,y'|\epsilon) = \int_{-\infty}^{\infty}\frac{dk}{2\pi}e^{ik(y-y')}\frac{\mathbf{g}^{\pm}}{(\epsilon - \frac{\hbar^2k^2}{2m^*}) - (\alpha^2+\beta^2)k^2 \pm i\delta sign(\epsilon - \frac{\hbar^2k^2}{2m^*})}, \tag{26}$$

where

$$\mathbb{G}^{\pm} = \begin{pmatrix}G^{\pm}_{\uparrow,\uparrow} & G^{\pm}_{\uparrow,\downarrow}\\ G^{\pm}_{\downarrow,\uparrow} & G^{\pm}_{\downarrow,\downarrow}\end{pmatrix}, \quad \text{and} \quad \mathbf{g}^{\pm} = \begin{pmatrix}\epsilon - \frac{\hbar^2k^2}{2m^*} & (\alpha+i\beta)k\\ (\alpha-i\beta)k & \epsilon - \frac{\hbar^2k^2}{2m^*}\end{pmatrix}. \tag{27}$$

We will integrate and express the "bare" Green's functions in the coordinate space. To this end, we calculate each component of the Green's function separately,

$$\begin{aligned}G^{\pm}_{\uparrow,\uparrow}(y,y'|\epsilon) &= \int_{-\infty}^{\infty}\frac{dk}{2\pi}e^{ik(y-y')} \\ &\times \frac{\epsilon - \frac{\hbar^2k^2}{2m^*}}{[\epsilon - \frac{\hbar^2k^2}{2m^*} + \sqrt{\alpha^2+\beta^2}\ |k| \pm i\delta][\epsilon - \frac{\hbar^2k^2}{2m^*} - \sqrt{\alpha^2+\beta^2}\ |k| \pm i\delta]} \\ &= -\frac{m^*}{2\pi\hbar^2}\int_{-\infty}^{\infty}dke^{ik(y-y')}\left\{\frac{1}{\left(k - \frac{m^*\tilde{\alpha}}{\hbar^2}\right)^2 - \frac{2m^*\epsilon}{\hbar^2} - \left(\frac{m^*\tilde{\alpha}}{\hbar^2}\right)^2 \mp i\delta}\right. \\ &\left. + \frac{1}{\left(k + \frac{m^*\tilde{\alpha}}{\hbar^2}\right)^2 - \frac{2m^*\epsilon}{\hbar^2} - \left(\frac{m^*\tilde{\alpha}}{\hbar^2}\right)^2 \mp i\delta}\right\},\end{aligned} \tag{28}$$

where $\tilde{\alpha} = \sqrt{\alpha^2+\beta^2}$. We replace the variable $\kappa = k - m^*\tilde{\alpha}/\hbar^2$ under the integrand, and take the integral by using the residue theorem. In this case, we have to consider two different cases: (i) $y - y' > 0$ and (ii) $y - y' < 0$. The result is written

$$G^{\pm}_{\uparrow,\uparrow}(y,y'|\epsilon) = \mp\frac{i}{v_F^*\hbar}\cos\left[\frac{m^*\tilde{\alpha}}{\hbar^2}(y-y')\right]e^{\pm i\frac{P_F^*}{\hbar}|y-y'|}, \tag{29}$$

where $P_F^* = \sqrt{2m^*\epsilon + (m^*\tilde{\alpha})^2}$ and $v_F^* = P_F^*/m^* = \sqrt{2\epsilon/m^* + m^*(\tilde{\alpha})^2}$. It is clear that

$$G^{\pm}_{\downarrow,\downarrow}(y,y'|\epsilon) = G^{\pm}_{\uparrow,\uparrow}(y,y'|\epsilon). \tag{30}$$

Now, we calculate the non-diagonal components of the Green's function.

$$\begin{aligned}G^{\pm}_{\uparrow,\downarrow}(y,y'|\epsilon) &= \int_{-\infty}^{\infty}\frac{dk}{2\pi}e^{ik(y-y')} \\ &\times \frac{(\alpha+i\beta)k}{[\epsilon - \frac{\hbar^2k^2}{2m^*} + \sqrt{\alpha^2+\beta^2}\ |k| \pm i\delta][\epsilon - \frac{\hbar^2k^2}{2m^*} - \sqrt{\alpha^2+\beta^2}\ |k| \pm i\delta]} \\ &= -\frac{m^*}{2\pi\hbar^2}\sqrt{\frac{\alpha+i\beta}{\alpha-i\beta}}\int_{-\infty}^{\infty}dke^{ik(y-y')} \\ &\times\left\{\frac{1}{\left(k - \frac{m^*\tilde{\alpha}}{\hbar^2}\right)^2 - \frac{2m^*\epsilon}{\hbar^2} - \left(\frac{m^*\tilde{\alpha}}{\hbar^2}\right)^2 \mp i\delta}\right. \\ &\left. + \frac{1}{\left(k + \frac{m^*\tilde{\alpha}}{\hbar^2}\right)^2 - \frac{2m^*\epsilon}{\hbar^2} - \left(\frac{m^*\tilde{\alpha}}{\hbar^2}\right)^2 \mp i\delta}\right\},\end{aligned} \tag{31}$$

By applying the same procedure that we used in calculation of the integral in Eq. (28), we get the expression

$$G^{\pm}_{\uparrow,\downarrow}(y,y'|\epsilon) = \mp\frac{1}{v_F^*\hbar}\sqrt{\frac{\alpha+i\beta}{\alpha-i\beta}}\sin\left[\frac{m^*\tilde{\alpha}}{\hbar^2}(y-y')\right]e^{\pm i\frac{P_F^*}{\hbar}|y-y'|}. \tag{32}$$

and

$$G^{\pm}_{\downarrow,\uparrow}(y,y'|\epsilon) = \mp\frac{1}{v_F^*\hbar}\sqrt{\frac{\alpha-i\beta}{\alpha+i\beta}}\sin\left[\frac{m^*\tilde{\alpha}}{\hbar^2}(y-y')\right]e^{\pm i\frac{P_F^*}{\hbar}|y-y'|}. \tag{33}$$

4. The diagrammatic method of Berezinskii in the presence of Rashba- and Dresselhaus SOIs

We write the Green's function as 2×2 matrix. This matrix can be decomposed as a multiplication of two matrices as

$$\mathbb{G}^{\pm}(y,y'|\epsilon) = \mp\frac{i}{2v_F^*\hbar}e^{\pm i\frac{p_F^*}{\hbar}|y-y'|}\begin{pmatrix} e^{i\frac{m^*\tilde{\alpha}}{\hbar^2}y}, & e^{-i\frac{m^*\tilde{\alpha}}{\hbar^2}y} \\ -\sqrt{\frac{\alpha-i\beta}{\alpha+i\beta}}e^{i\frac{m^*\tilde{\alpha}}{\hbar^2}y}, & \sqrt{\frac{\alpha-i\beta}{\alpha+i\beta}}e^{-i\frac{m^*\tilde{\alpha}}{\hbar^2}y}\end{pmatrix} \times\begin{pmatrix} e^{-i\frac{m^*\tilde{\alpha}}{\hbar^2}y'}, & -\sqrt{\frac{\alpha+i\beta}{\alpha-i\beta}}e^{-i\frac{m^*\tilde{\alpha}}{\hbar^2}y'} \\ e^{i\frac{m^*\tilde{\alpha}}{\hbar^2}y'}, & \sqrt{\frac{\alpha+i\beta}{\alpha-i\beta}}e^{i\frac{m^*\tilde{\alpha}}{\hbar^2}y'}\end{pmatrix} \tag{34}$$

The Green's function in the matrix form is again factorizable, as it is in the conventional Berezinskii's technique. Nevertheless, in difference from the conventional technique, now the Green's function depends on the direction and we cannot order the impurity coordinates. After beaking up the coordinate-dependent factors and transferring them to the vertices y and y', the coordinate dependence of the Green's function is transferred from the line to the vertex. We now draw all possible vertices and calculate them. Fig. 1 shows all possible internal vertices giving a contribution to the correlators. Let us calculate in detail the internal impurity vertices a (a') and e

$$\begin{aligned}(a\ (a')) &= c_{imp}\left(\frac{-i}{2\hbar v_F^*}\right)^2\begin{pmatrix} e^{iy}, & e^{-iy} \\ -\sqrt{\frac{-}{+}}e^{iy}, & \sqrt{\frac{-}{+}}e^{-iy}\end{pmatrix}\begin{pmatrix} e^{-iy}, & -\sqrt{\frac{+}{-}}e^{-iy} \\ e^{iy}, & \sqrt{\frac{+}{-}}e^{-iy}\end{pmatrix} \times\begin{pmatrix} V, & 0 \\ 0, & V\end{pmatrix} \\ &\begin{pmatrix} e^{iy}, & e^{-iy} \\ -\sqrt{\frac{-}{+}}e^{iy}, & \sqrt{\frac{-}{+}}e^{-iy}\end{pmatrix}\begin{pmatrix} e^{-iy}, & -\sqrt{\frac{+}{-}}e^{-iy} \\ e^{iy}, & \sqrt{\frac{+}{-}}e^{-iy}\end{pmatrix}\begin{pmatrix} V, & 0 \\ 0, & V\end{pmatrix} \\ &= -c_{imp}\left(\frac{1}{\hbar v_F^*}\right)^2 V_0 I_0 \\ &= -\frac{1}{l_{SO}^+}I_0,\end{aligned} \tag{35}$$

$$\begin{aligned}(e) &= c_{imp}\left(\frac{-i}{2\hbar v_F^*}\right)\left(\frac{i}{2\hbar v_F^*}\right)e^{2i\frac{p_F^{*\prime}-p_F^*}{\hbar}y}\begin{pmatrix} e^{iy}, & e^{-iy} \\ -\sqrt{\frac{-}{+}}e^{iy}, & \sqrt{\frac{-}{+}}e^{-iy}\end{pmatrix} \times\begin{pmatrix} e^{-iy}, & -\sqrt{\frac{+}{-}}e^{-iy} \\ e^{iy}, & \sqrt{\frac{+}{-}}e^{-iy}\end{pmatrix}\begin{pmatrix} V, & 0 \\ 0, & V\end{pmatrix} \\ &\begin{pmatrix} e^{iy}, & e^{-iy} \\ -\sqrt{\frac{-}{+}}e^{iy}, & \sqrt{\frac{-}{+}}e^{-iy}\end{pmatrix}\begin{pmatrix} e^{-iy}, & -\sqrt{\frac{+}{-}}e^{-iy} \\ e^{iy}, & \sqrt{\frac{+}{-}}e^{-iy}\end{pmatrix}\begin{pmatrix} V, & 0 \\ 0, & V\end{pmatrix} \\ &= c_{imp}\left(\frac{e^{i\frac{\omega}{\hbar v_F^*}y}}{\hbar v_F^*}\right)^2 V_0 I_0 \\ &= \frac{e^{2i\frac{\omega}{\hbar v_F^*}y}}{l_{SO}^-}I_0,\end{aligned} \tag{36}$$

where we use the following shortcut: $e^{\pm iy}$ instead of $e^{\pm i\frac{m^*\tilde{\alpha}}{\hbar^2}y}$ and $\sqrt{\frac{\pm}{\mp}}$ instead of $\sqrt{\frac{\alpha\pm i\beta}{\alpha\mp i\beta}}$; $I_0 = \begin{pmatrix} 1, & 0 \\ 0, & 1\end{pmatrix}$, $p_F^{*\prime} - p_F^* = \sqrt{2m^*(\epsilon+\omega)+(m^*\tilde{\alpha})^2} - \sqrt{2m^*\epsilon+(m^*\tilde{\alpha})^2} \approx \frac{\omega}{v_F^*}$ for small external frequency ω. V_0 in the above expressions corresponds to the correlator of the impurity potential. For the white-noise Gaussian random potential $\langle V(y)\rangle = 0$ and $V(y-y') = \langle V(y)V(y')\rangle = c_{imp}V_0\delta(y-y')/\hbar^2 v_F^{*2} \equiv l^{-1}\delta(x-x')$, where the mean-free path is defined as $l^{-1} = (l_{SO}^{\pm})^{-1} = c_{imp}V_0/\hbar^2 v_F^{*2}$. All other internal vertices are calculated in a similar way and give the following results:

$$\begin{aligned}&(b\ (b')) = -I_0/2l_{SO}^- - I_0/2l_{SO}^+; \quad (c\ (c')) = -I_0/l_{SO}^-; \quad (d) = I_0/l_{SO}^+; \\ &(f) = \frac{e^{-2i\frac{\omega}{\hbar v_F^*}y}}{l_{SO}^-}I_0.\end{aligned} \tag{37}$$

It is necessary to note here that although we used the white-noise potential in these calculations, it is possible to generalize the random potential within the Born approximation, where the impurity potential correlator should not be proportional to δ-function. The potential is considered to be weak enough and does not overlap each other. This means that the width b of a single impurity potential is much smaller than the average distance c_{imp}^{-1} between the impurities. The mean free path is the largest distance scale $b \ll c_{imp}^{-1} \ll l$ within the Born approximation, and the impurity potential is characterized by the correlator of a width of order b

$$V(y-y') = \left\langle V(y)V(y')\right\rangle. \tag{38}$$

The impurity vertices become vertical lines, as they are in the case of δ-correlated white-noise potential, after integration over the internal variables $y-y'$, which yields the following expression for the essential vertices

$$\begin{aligned}\frac{1}{l_{SO}^+} &= \frac{2}{v_F^{*2}}\int_0^\infty U(y)dy; \qquad \text{and} \\ \frac{1}{l_{SO}^-} &= \frac{2}{v_F^{*2}}\int_0^\infty U(y)\cos\left[2p_F^*(\epsilon)y\right]dy.\end{aligned} \tag{39}$$

The parameters l_{SO}^- and l_{SO}^+ can be interpreted as the mean free paths of backward and forward scatterings, correspondingly. The main argument in the selection of the internal vertices, given in Fig. 1, is that these vertices do not contain strongly oscillating factor of the type $\exp(ik_F y_j)$. The vertices containing such kind of strongly oscillating factor give a small contribution, in the parameter of selection $k_F l \gg 1$ or $\epsilon\tau_- \gg 1$ for weak randomness, after integration over y_j. The external vertices, depicted in Fig. 2 contain the factor $\exp(i\omega y/v)$, which does not oscillate strongly for the frequency of an external field, satisfying the condition $\omega \ll \epsilon$. The following expression corresponds to the external vertex (a) in Fig. 2

$$\begin{aligned}(a) &= \sqrt{\frac{-i}{2\hbar v_F^*}}\sqrt{\frac{i}{2\hbar v_F^*}}e^{-i\frac{p_F^{*\prime}-p_F^*}{\hbar}y'}\begin{pmatrix} e^{-iy'}, & -\sqrt{\frac{+}{-}}e^{-iy'} \\ e^{iy'}, & \sqrt{\frac{+}{-}}e^{-iy'}\end{pmatrix} \\ &\times\begin{pmatrix} e^{iy'}, & e^{-iy'} \\ -\sqrt{\frac{-}{+}}e^{iy'}, & \sqrt{\frac{-}{+}}e^{-iy'}\end{pmatrix} = \frac{e^{-i\frac{\omega}{\hbar v_F^*}y'}}{\hbar v_F^*}I_0.\end{aligned} \tag{40}$$

All other external vertices are calculated in a similar way and have the form:

$$(b) = \frac{e^{i\frac{\omega}{\hbar v_F^*}y'}}{\hbar v_F^*}I_0; \quad (c) = \frac{e^{-i\frac{\omega}{\hbar v_F^*}y}}{\hbar v_F^*}I_0; \quad (d) = \frac{e^{i\frac{\omega}{\hbar v_F^*}y}}{\hbar v_F^*}I_0. \tag{41}$$

The calculations show that all possible impurity vertices do not differ from those given in Ref. Berezinskii [30], except that they are written in a 2×2 matrix form and the Fermi velocity v_F^* now depends on the SO coupling constants.

5. Electron density distribution

Behavior of the density–density correlator $\chi^0(y-y';t-t')$ at large time $|t-t'| \gg \tau_0$ and distance $|y-y'| \gg l_{SO}^-$ describes character of the localization. The large time scale corresponds to low frequency case $\nu = 2\omega\tau_0 \gg 1$, where the diagrams with large $m \approx \nu^{-1} \gg 1$ give main contribution to the correlators. This limit allows to transform the discrete difference equations, Eqs. (45)–(51), to the differential

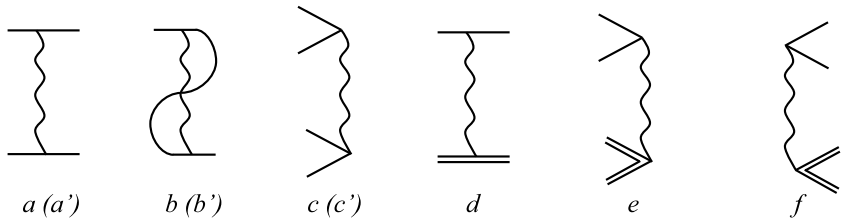

Fig. 1. The possible internal impurity vertices given contribution in the weak randomness limit $\epsilon_F \tau \gg 1$. Single- and double-lines correspond to the retarded- and advanced Green's functions. The wavy-line shows the impurity vertex for the random potential. Vertices a', b' and c' differ from a, b and c by replacing the single lines by double lines.

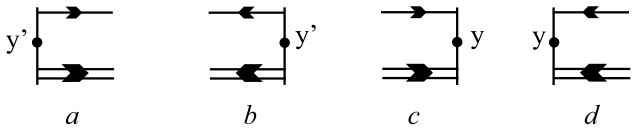

Fig. 2. The possible external vertices giving contribution to the essential diagrams.

equations in term of continuous variable $p = -i\nu m$. Routine calculations show that $\chi^0(y,t)$ yields a stationary distribution as $t \to \infty$

$$p_\infty(y) = \chi^0(y,t)|_{t\to\infty} \approx \left(\frac{\pi}{16}\right)^{\frac{3}{2}} \frac{1}{4l_{SO}^-} \left(\frac{4l_{SO}^-}{|y|}\right)^{3/2} \exp\left(-\frac{|y|}{4l_{SO}^-}\right). \tag{42}$$

The distribution is depicted in Fig. 3. Four different cases, $\frac{l_{SO}}{l_0} = \frac{(m^*\tilde{\alpha})^2}{2\epsilon} = 0; 0.5; 1$ and 1.5, are presented in Fig. 3 by solid (red), dashed (cyan), dot-dashed (blue) and dotted (orange) curves, correspondingly, where $l_{SO}^- = l_0 + l_{SO}$ and $l_0 = \frac{2\hbar^2\epsilon}{c_{imp}V_0 m^*}, l_{SO} = \frac{\hbar^2 m^* \tilde{\alpha}^2}{c_{imp}V_0}$. The exponential decay of the distribution function clearly shows that even two impurities are enough to localize an electron in the $1D$ disordered system, and the localization length $l_{loc} = 4l_{SO}^-$. It is seen from the figure that the peak becomes smaller with increasing $\tilde{\alpha}$. This feature demonstrates that the Rashba and Dresselhaus SO terms equally and independently contribute to the localized state.

6. Conclusions

In this work, we study the effect of randomly distributed impurities in a one-dimensional wire in the presence of Rashba and Dresselhaus SO interactions. For this purpose, we constructed a diagrammatic method as an extension of the Berezinskii technique to the problem with spin–orbit interaction. It is worthy to notice that the results in this work are not pure academic ones, but they can be used to understand and to interpret the experimental measurements on a single dislocation and on Si(557)-Au, Si(553)-Au and other Au chain structures on vicinal Si(111). Indeed, core of a dislocation consists of dangling bonds. Strong deformation potential around the dislocation core attracts the impurities, forming an impurity 'cloud' around the dislocation core. The potential derivative in the radial direction is nonzero, which is a source of the Rashba SO coupling in a single dislocation.

Declaration of competing interest

The authors declare that they have no known competing financial interests or personal relationships that could have appeared to influence the work reported in this paper.

Data availability

No data was used for the research described in the article.

Acknowledgments

BT is partially supported by The Scientific and Technological Research Council of Turkey (TUBITAK) and Turkish Academy of Sciences (TUBA).

Appendix. Derivation of the correlators

For $y > y'$ a diagram for the average value of the correlator $G^+(y,y'|\epsilon+\omega)G^-(y',y|\epsilon)$ can be subdivided into three parts: right (to the right of y), central (between y and y'), and left (to the left of y') part. We denote the sum of the right-parts (left-parts) of all possible diagrams, having $2m$ single- and $2m$ double-lines in the cross-section by $R_m(y)$ ($L_m(y')$), and the sum of the central parts of all diagrams by $Z_{m',m}(y',y)$. The selected vertices have such symmetry that they either do not change the number of both single and double lines or change the number of the lines symmetrically $\Delta m = \Delta m' = \pm 1$. The right-part of the diagrams can be constructed by successively joining all internal vertices in Fig. 1 to the right of already constructed right-part [30,34]

$$-\frac{d}{dy}R_m(y) = \frac{1}{l_{SO}^-}\left\{m^2 R_{m-1}(y)e^{2i\omega y/v_F^*} + m^2 R_{m+1}(y)e^{-2i\omega y/v_F^*} - 2m^2 R_m(y)\right\}. \tag{43}$$

Equation for the right-part $R_m(y)$ and left-part $R_{m'}(y')$ are simplified after replacements

$$R_m(y) = R_m e^{2im\omega y/v_F^*}, \quad \text{and} \quad R_{m'}(y') = R_{m'}e^{-2im'\omega y'/v_F^*}, \tag{44}$$

where R_m and $R_{m'}$ obey the same equation

$$i\nu m R_m + m^2\left(R_{m+1} + R_{m-1} - 2R_m\right) = 0 \tag{45}$$

with the boundary condition $R_0 = 1$ and $\nu = 2\omega\tau_-$.

The equation for the central part $Z_{m',m}(y',y)$ reads

$$\frac{d}{dy}Z_{m',m}(y',y) = \frac{i\omega}{v}Z_{m',m}(y',y) + \frac{1}{l_{SO}^-}\left\{m^2 Z_{m',m-1}e^{-2i\omega y/v_F^*} + (m+1)^2 Z_{m',m+1}e^{2i\omega y/v_F^*} - \left[2m^2 + (m+1)^2\right]Z_{m',m}(y',y)\right\}. \tag{46}$$

Subscript m (m') in the central part show that there are $2m+1$ ($2m'+1$) single and double lines in the cross-section at y_{-0} (y'_{+0}). The boundary condition for $Z_{m',m}(y',y)$ as $y \to y'+0$

$$Z_{m',m}(y',y'+0) = \delta_{m',m}. \tag{47}$$

Left-, central- and right-parts are combined and summed up for each pair of the external vertices. Final expression for the correlators can be shown

$$\chi^a(k,\omega) = \frac{2l_{SO}^-}{\pi}\sum_m P_m^a(\omega)\left\{Q_m^a(k,\omega) + Q_m^a(-k,\omega)\right\}, \tag{48}$$

where

$$P_m^0(\omega) = \frac{1}{2}(R_m + R_{m+1}); \quad \text{and} \quad P_m^1(\omega) = R_m - R_{m+1}. \tag{49}$$

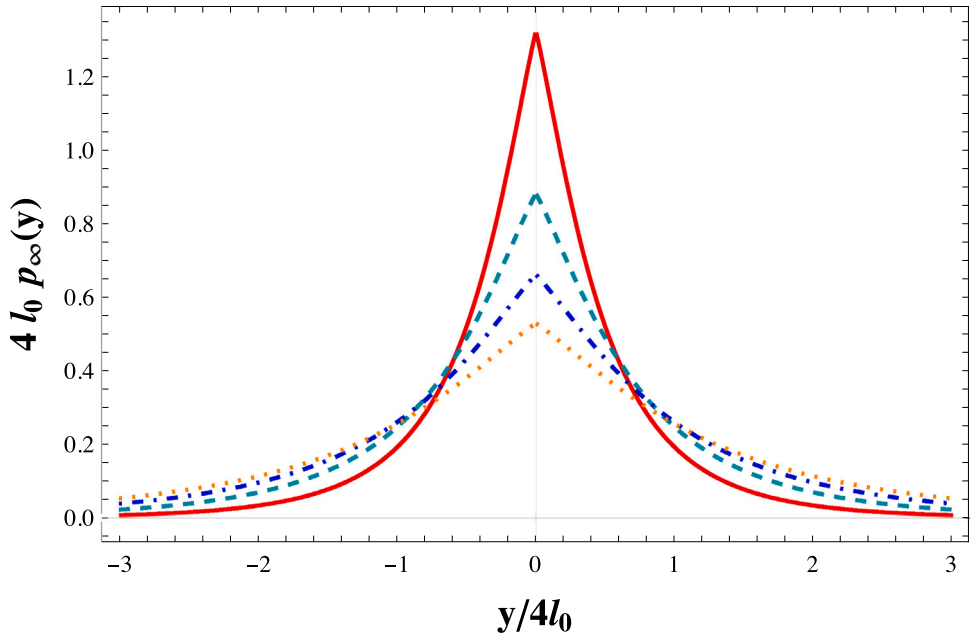

Fig. 3. Distribution of the electron density $p_\infty(y)$ in the localized state for $|y| \gg l_{SO}^-$.

The central part is replaced by new block Q_m by means of the following transformation

$$Q_m^a(k,\omega) = \frac{1}{4l_{SO}^-}\sum_{m'=0}^{\infty}\int_{y'}^{\infty} dy e^{ik(y'-y)} e^{-2i\omega m' y'/v_F^*} Z_{m',m}(y',y) e^{2i\omega m y/v_F^*} P_{m'}^a, \tag{50}$$

and obeys the recurrence equation

$$iv\left(m+\frac{1}{2}\right)Q_m^a + (m+1)^2\left(Q_{m+1}^a - Q_m^a\right) - m^2\left(Q_m^a - Q_{m-1}^a\right) - i\kappa Q_m^a + P_m^a = 0, \tag{51}$$

where $\kappa = kl_{SO}^-$. Solution of Eqs. (45), (51) with (48) allows to calculate the expression for the density–density (13) and charge–charge (14) correlators.

References

[1] J.-i. Inoue, G.E.W. Bauer, L.W. Molenkamp, Diffuse transport and spin accumulation in a Rashba two-dimensional electron gas, Phys. Rev. B 67 (3) (2003) 033104, http://dx.doi.org/10.1103/PhysRevB.67.033104, URL: https://link.aps.org/doi/10.1103/PhysRevB.67.033104.

[2] A.A. Burkov, A.S. Núñez, A.H. MacDonald, Theory of spin-charge-coupled transport in a two-dimensional electron gas with Rashba spin-orbit interactions, Phys. Rev. B 70 (15) (2004) 155308, http://dx.doi.org/10.1103/PhysRevB.70.155308, URL: https://link.aps.org/doi/10.1103/PhysRevB.70.155308.

[3] J. Schliemann, D. Loss, Dissipation effects in spin-hall transport of electrons and holes, Phys. Rev. B 69 (16) (2004) 165315, http://dx.doi.org/10.1103/PhysRevB.69.165315, URL: https://link.aps.org/doi/10.1103/PhysRevB.69.165315.

[4] E.G. Mishchenko, A.V. Shytov, B.I. Halperin, Spin current and polarization in impure two-dimensional electron systems with spin-orbit coupling, Phys. Rev. Lett. 93 (22) (2004) 226602, http://dx.doi.org/10.1103/PhysRevLett.93.226602, URL: https://link.aps.org/doi/10.1103/PhysRevLett.93.226602.

[5] A.V. Moroz, C.H.W. Barnes, Effect of the spin-orbit interaction on the band structure and conductance of quasi-one-dimensional systems, Phys. Rev. B 60 (20) (1999) 14272–14285, http://dx.doi.org/10.1103/PhysRevB.60.14272, URL: https://link.aps.org/doi/10.1103/PhysRevB.60.14272.

[6] W. Häusler, Rashba precession in quantum wires with interaction, Phys. Rev. B 63 (12) (2001) 121310, http://dx.doi.org/10.1103/PhysRevB.63.121310, URL: https://link.aps.org/doi/10.1103/PhysRevB.63.121310.

[7] P. Středa, P. Šeba, Antisymmetric spin filtering in one-dimensional electron systems with uniform spin-orbit coupling, Phys. Rev. Lett. 90 (25) (2003) 256601, http://dx.doi.org/10.1103/PhysRevLett.90.256601, URL: https://link.aps.org/doi/10.1103/PhysRevLett.90.256601.

[8] A. Reynoso, G. Usaj, M.J. Sánchez, C.A. Balseiro, Theory of edge states in systems with Rashba spin-orbit coupling, Phys. Rev. B 70 (23) (2004) 235344, http://dx.doi.org/10.1103/PhysRevB.70.235344, URL: https://link.aps.org/doi/10.1103/PhysRevB.70.235344.

[9] S. Kettemann, Dimensional control of antilocalization and spin relaxation in quantum wires, Phys. Rev. Lett. 98 (17) (2007) 176808, http://dx.doi.org/10.1103/PhysRevLett.98.176808, URL: https://link.aps.org/doi/10.1103/PhysRevLett.98.176808.

[10] C. De Grandi, V. Gritsev, A. Polkovnikov, Quench dynamics near a quantum critical point, Phys. Rev. B 81 (1) (2010) 012303, http://dx.doi.org/10.1103/PhysRevB.81.012303, URL: https://link.aps.org/doi/10.1103/PhysRevB.81.012303.

[11] M. Kittler, M. Reiche, in: S. Basu (Ed.), Structure and Properties of Dislocations in Silicon, IntechOpen, London, 2011.

[12] I. Yonenaga, in: D. Yang (Ed.), Defects in Crystalline Silicon: Dislocations, Springer Berlin Heidelberg, Berlin, Heidelberg, 2019, pp. 1–48, http://dx.doi.org/10.1007/978-3-662-52735-1{_}24-1.

[13] A.N. Mihalyuk, J.P. Chou, S.V. Eremeev, A.V. Zotov, A.A. Saranin, One-dimensional Rashba states in Pb atomic chains on a semiconductor surface, Phys. Rev. B 102 (3) (2020) 035442, http://dx.doi.org/10.1103/PhysRevB.102.035442, URL: https://link.aps.org/doi/10.1103/PhysRevB.102.035442.

[14] A.G. Syromyatnikov, S.V. Kolesnikov, A.M. Saletsky, A.L. Klavsyuk, Formation and properties of metallic atomic chains and wires, Phys.-Usp. 64 (2021) 671.

[15] F.E. Meijer, A.F. Morpurgo, T.M. Klapwijk, One-dimensional ring in the presence of Rashba spin-orbit interaction: Derivation of the correct Hamiltonian, Phys. Rev. B 66 (3) (2002) 033107, http://dx.doi.org/10.1103/PhysRevB.66.033107, URL: https://link.aps.org/doi/10.1103/PhysRevB.66.033107.

[16] S. Souma, B.K. Nikolić, Spin hall current driven by quantum interferences in mesoscopic Rashba rings, Phys. Rev. Lett. 94 (10) (2005) 106602, http://dx.doi.org/10.1103/PhysRevLett.94.106602, URL: https://link.aps.org/doi/10.1103/PhysRevLett.94.106602.

[17] Z. Zhi-Yong, Spin accumulation on a one-dimensional mesoscopic Rashba ring, J. Phys.: Condens. Matter 18 (2006) 4101.

[18] M. Niţă, D.C. Marinescu, A. Manolescu, B. Ostahie, V. Gudmundsson, Persistent oscillatory currents in a 1D ring with Rashba and Dresselhaus spin–orbit interactions excited by a terahertz pulse, Physica E 46 (2012) 12–20, http://dx.doi.org/10.1016/j.physe.2012.08.017, URL: https://www.sciencedirect.com/science/article/pii/S1386947712003232.

[19] Y. Gindikin, V.A. Sablikov, Image-potential-induced spin-orbit interaction in one-dimensional electron systems, Phys. Rev. B 95 (4) (2017) 045138, http://dx.doi.org/10.1103/PhysRevB.95.045138, URL: https://link.aps.org/doi/10.1103/PhysRevB.95.045138.

[20] J. Yuan, Y. Cai, L. Shen, Y. Xiao, J.-C. Ren, A. Wang, Y.P. Feng, X. Yan, One-dimensional thermoelectrics induced by Rashba spin-orbit coupling in two-dimensional BiSb monolayer, Nano Energy 52 (2018) 163–170, http://dx.doi.org/10.1016/j.nanoen.2018.07.041, URL: https://www.sciencedirect.com/science/article/pii/S2211285518305305.

[21] P. Segovia, D. Purdie, M. Hengsberger, Y. Baer, Observation of spin and charge collective modes in one-dimensional metallic chains, Nature 402 (6761) (1999) 504–507, http://dx.doi.org/10.1038/990052.

[22] F. Massel, A. Kantian, J. Daley, T. Giamarchim, P. Törmä, Dynamics of an impurity in a one-dimensional lattice, New J. Phys. 15 (2013) 045018.

[23] I. Barke, F. Zheng, T.K. Rügheimer, F.J. Himpsel, Experimental evidence for spin-split bands in a one-dimensional chain structure, Phys. Rev. Lett. 97 (22) (2006) 226405, http://dx.doi.org/10.1103/PhysRevLett.97.226405, URL: https://link.aps.org/doi/10.1103/PhysRevLett.97.226405.

[24] E. Abrahams, P.W. Anderson, D.C. Licciardello, T.V. Ramakrishnan, Scaling theory of localization: Absence of quantum diffusion in two dimensions, Phys. Rev. Lett. 42 (10) (1979) 673–676, http://dx.doi.org/10.1103/PhysRevLett.42.673, URL: https://link.aps.org/doi/10.1103/PhysRevLett.42.673.

[25] N.F. Mott, W.D. Twose, The theory of impurity conduction, Adv. Phys. 10 (38) (1961) 107–163, http://dx.doi.org/10.1080/00018736100101271.

[26] R.E. Borland, J.A. Pople, The nature of the electronic states in disordered one-dimensional systems, Proc. R. Soc. Lond. Ser. A Math. Phys. Eng. Sci. 274 (1359) (1963) 529–545, http://dx.doi.org/10.1098/rspa.1963.0148.

[27] B.I. Halperin, Green's functions for a particle in a one-dimensional random potential, Phys. Rev. 139 (1A) (1965) A104–A117, http://dx.doi.org/10.1103/PhysRev.139.A104, URL: https://link.aps.org/doi/10.1103/PhysRev.139.A104.

[28] N.F. Mott, Conduction in non-crystalline systems, Philos. Mag. J. Theor. Exp. Appl. Phys. 22 (175) (1970) 7–29, http://dx.doi.org/10.1080/14786437008228147.

[29] N.F. Mott, E.A. Davis, Electronic processes in non-crystalline materials, 1979.

[30] V.L. Berezinskii, Kinetics of a quantum particle in a one-dimesional random potential, Sov. Phys.—JETP 38 (3) (1974) 620–627.

[31] B. Suleymanli, E. Nakhmedov, O. Alekperov, F. Tatardar, B. Tanatar, Motion of two-dimensional quantum particle under a linear potential in the presence of Rashba and Dresselhaus spin–orbit interactions, Solid State Commun. 342 (2022) 114582, http://dx.doi.org/10.1016/j.ssc.2021.114582, URL: https://www.sciencedirect.com/science/article/pii/S0038109821003665.

[32] C.L. Romano, S.E. Ulloa, P.I. Tamborenea, Level structure and spin-orbit effects in quasi-one-dimensional semiconductor nanostructures, Phys. Rev. B 71 (3) (2005) 035336, http://dx.doi.org/10.1103/PhysRevB.71.035336, URL: https://link.aps.org/doi/10.1103/PhysRevB.71.035336.

[33] S. Datta, B. Das, Electronic analog of the electro-optic modulator, Appl. Phys. Lett. 56 (7) (1990) 665–667, http://dx.doi.org/10.1063/1.102730.

[34] A.A. Gogolin, Electron localization and hopping conductivity in one-dimensional disordered systems, Phys. Rep. 86 (1) (1982) 1–53, http://dx.doi.org/10.1016/0370-1573(82)90069-2, URL: https://www.sciencedirect.com/science/article/pii/0370157382900692.